Neurochemistry International 128 (2019) 85–93

Contents lists available at ScienceDirect

Neurochemistry International

journal homepage: www.elsevier.com/locate/neuint

Streptozotocin causes acute responses on hippocampal S100B and BDNF proteins linked to glucose metabolism alterations

Leticia Rodrigues*,[1], Krista Minéia Wartchow[1], Lucas Zingano Suardi, Barbara Carolina Federhen, Nicholas Guerini Selistre, Carlos-Alberto Gonçalves

Department of Biochemistry, Universidade Federal do Rio Grande do Sul, Porto Alegre, Brazil

ARTICLE INFO

Keywords:
BDNF
Glucose metabolism
Hippocampus
Streptozotocin
S100B

ABSTRACT

Streptozotocin (STZ) is a glucosamine-nitrosourea commonly used to induce long-lasting models of diabetes mellitus and Alzheimer's disease. Direct toxicity of STZ on the pancreas and kidneys has been well characterized, but the acute effect of this compound on brain tissue has received less attention. Herein, we investigated the acute and direct toxicity of STZ on fresh hippocampal slices, measuring changes in BDNF and S100B secretion (two widely-used peripheral markers of brain injury), as well as glucose metabolism. Moreover, we investigated *in vivo* changes of these proteins in the hippocampus, 48 h after intracerebroventricular STZ administration. Transverse hippocampal slices (0.3 mm thick) were obtained using a McIlwain tissue chopper and target proteins were measured in the incubation medium by ELISA. STZ decreased S100B secretion, but increased BDNF secretion as well as causing impairment in glucose uptake in hippocampal slices, measured using [^{3}H] deoxyglucose. Glucose levels and glucose metabolism differentially modulated S100B secretion in astrocytes and BDNF secretion in neurons, when evaluated under specific conditions (high-potassium medium, presence of tetrodotoxin or fluorocitrate). Moreover, at 48 h after intracerebroventricular STZ, hippocampal BDNF content, but not S100B, was reduced. Our results indicate that BDNF and S100B are useful and sensitive markers of glucose metabolism disturbance and reinforce these proteins as general acute markers of brain disorders.

1. Introduction

Streptozotocin (STZ) is a glucosamine-nitrosourea compound produced by the *Streptomyces achromogenes* bacteria and is currently used to treat some types of endocrine tumors (Okusaka et al., 2015). Its action appears to be dependent upon the glucose transporter type 2 (GLUT2). Experimentally, STZ is used to induce diabetes mellitus (DM), types 1 and 2, due to its high toxicity to pancreas tissue, which affects glucose metabolism and insulin secretion (Chen and Zhong, 2013; Okusaka et al., 2015). Once inside the pancreatic beta cell, STZ causes DNA alkylation and, consequently, cell death (Bennett and Pegg, 1981). The *in vitro* and acute *in vivo* toxicity of STZ on the pancreas and kidneys has been well characterized (Eizirik et al., 1993; Katakam et al., 2005; Harb et al., 2007; Rosenberger et al., 2008; Brouwers et al., 2013).

A subdiabetogenic dosage of STZ was first used in the 1990's to produce a sporadic Alzheimer's disease (AD) model in rodents by intracerebroventricular (ICV) administration (Hoyer et al., 1994; Frölich et al., 1998; Lannert and Hoyer, 1998). This model reproduces several AD characteristics, including glucose hypometametabolism, and has been widely used to investigate potential strategic therapies (Salkovic-Petrisic et al., 2013). The chronic effect of STZ toxicity on brain tissue has been investigated at weeks or months after ICV administration and in particular to investigate cognitive deficit and long-term neurochemical alterations (Rodrigues et al., 2009; Salkovic-Petrisic et al., 2013; Biasibetti et al., 2017).

The hippocampus is an important brain region for cognition, and cognitive deficits associated with hippocampal dysfunction have been characterized in many brain disorders, including in patients and STZ models of DM and AD (Nardin et al., 2016; Flores-Gómez et al., 2019). Moreover, some *in vitro* assays of STZ toxicity in brain tissue preparations suggest that acute and/or early changes are important for understanding long-lasting brain changes induced by this compound (Kraska et al., 2012; Ju et al., 2016; Knezovic et al., 2017; Souza et al., 2017).

Acute administration of STZ ICV induces an astrocytic response, as assessed by glial fibrillary astrocytic protein (GFAP) immunoreactivity,

* Corresponding author. Av Ramiro Barcelos, 2600-anexo, Laboratory of Calcium-Binding Proteins in CNS, Department of Biochemistry, Universidade Federal do Rio Grande do Sul, 90035-003, Porto Alegre, Brazil.
E-mail addresses: letigues@gmail.com, casg@ufrgs.br (L. Rodrigues).
[1] These authors share first authorship.

https://doi.org/10.1016/j.neuint.2019.04.013
Received 12 March 2019; Received in revised form 12 April 2019; Accepted 19 April 2019
Available online 20 April 2019

one hour after infusion as well as increased hippocampal GLUT2 expression and a decrease in insulin receptor (IR) expression (Knezovic et al., 2017). Another study investigated the effect of STZ ICV in mice one, six, twenty-four hours and one week after administration on depressive-like parameters, hippocampal cytokines and brain-derived neurotrophic factor (BDNF) levels (Souza et al., 2017).

BDNF is the most abundant brain neurotrophin (see Kowiański et al., 2018 for a review) and strongly associated with brain plasticity and energetic metabolism. Changes in the levels of this neurotrophin in the brain, as well as peripheral changes in plasma or serum have been associated with acute brain injury, neurodegenerative disease and psychiatric disorders (Fernandes et al., 2014; Serra-Millàs, 2016; Stanne et al., 2016). In STZ-induced type 2 DM, rats reportedly have reduced levels of BDNF in the brain tissue, liver and pancreas (Bathina et al., 2017; Bathina and Das, 2018). Hippocampal changes in BDNF levels have been observed under other toxic conditions, such as hyperammonemia (Galland et al., 2017), Pb exposure (Baranowska-Bosiacka et al., 2013), and excitotoxicity (Rosa et al., 2016). BDNF is produced mainly by neurons in brain tissue, but astrocytes are able to convert pro-BDNF, released by neurons, to BDNF (Bergami et al., 2008). However, under conditions of injury, astrocytes begin to express and release BDNF (Kimura et al., 2016).

S100B protein is an astrocyte marker of activation and/or brain damage in acute and chronic conditions (see Gonçalves et al., 2008 et al., 2008 for a review). The mechanism of S100B secretion remains unclear (Leite et al., 2017), but the neurotrophic and toxic effect of this protein appears to be mediated by RAGE, the receptor for advanced glycated end products and also beta-amyloid peptides (Donato, 2007). Recent findings suggest that S100B modulates glucose metabolism in the brain tissue (Wartchow et al., 2016).

Clinical and experimental studies have shown that several psychiatric disorders are associated with changes in glucose metabolism in the brain, and type 2 DM is a frequent comorbidity in bipolar disorder, schizophrenia e major depressive disorder (Regenold et al., 2002; Ohaeri and Akanji, 2011). Molecular imaging of glucose uptake by with ^{18}F-fluorodeoxy-glucose positron-emission tomography seems to be useful in the diagnosis of neuropsychiatric diseases, particularly in their early stages (Schöll et al., 2014). Changes in S100B and BDNF levels have also been described in these psychiatric diseases (Kalia and Costa E Silva, 2015; Dorofeikova et al., 2018) and it is possibly that these changes are linked to alterations in glucose metabolism.

Herein, we investigated the acute effect of STZ on hippocampal slices, measuring changes in BDNF and S100B secretion, two widely used markers for brain disorders, as well as glucose metabolism using ^{3}H-deoxy-glucose. Moreover, we investigated *in vivo* changes of these proteins the in hippocampus and CSF 48 h after ICV STZ administration.

2. Material and methods

2.1. Subjects

For the preparation of hippocampal slices and the STZ model, male 90-day-old Wistar rats were obtained from our breeding colony (Department of Biochemistry, UFRGS, Porto Alegre, Brazil). The animals were maintained under controlled light and environmental conditions (12 h light/12 h dark cycle at a constant temperature of 22 ± 1 °C) with free access to commercial chow and water.

2.2. Chemicals

Streptozotocin (STZ), Methylthiazolyldiphenyltetrazolium bromide (MTT), cytochalasin B (Cyt B), fluorocitrate (FC), tetrodotoxin (TTX), S100B protein, anti-S100B antibody (SH-B1), o-phenylenediamine (OPD) were purchased from Sigma-Aldrich (St. Louis, MO- USA). Polyclonal anti-S100B (clone SH-B) and anti-GFAP antibodies were purchased from Dako (São Paulo, Brazil). Anti-BDNF antibody was obtained from Santa Cruz Biotechnology (Santa Cruz, CA, USA). Peroxidase secondary antibodies were from GE (Little Chalfont, United Kingdom) and fluorescent from Alexa Fluor (Invitrogen). Deoxy-[3-^{3}H] glucose (20 Ci/mmol) was purchased from PerkinElmer (Boston, MA, USA). Other reagents were purchased from local commercial suppliers (Sulquímica or Labsul, Porto Alegre, Brazil).

2.3. Preparation and incubation of brain hippocampal slices

Rats were decapitated and their hippocampi were quickly dissected out. Transverse sections (0.3 mm) of tissue were rapidly obtained using a McIlwain tissue chopper. One slice was placed into each well of a 24-well culture plate. Slices were incubated in oxygenated physiological medium containing, in mM, 120 NaCl, 2.0 KCl, 1.0 $CaCl_2$, 1.0 $MgSO_4$, 25.0 Hepes, 1.0 KH_2PO_4 and 10.0 glucose, pH 7.4, at room temperature. The medium was changed every 15 min with fresh medium. Following a 120-min equilibration period, slices were incubated in medium in the presence/absence of treatment conditions for 1 h at 30 °C (Nardin et al., 2009).

2.4. Hippocampal slices treatments

To evaluate S100B, BDNF secretion and glucose uptake, hippocampal slices (1 slice/well) were treated with different concentrations of STZ (100 μM, 1 and 10 mM) for 1 h in 0.3 mL saline medium. In order to evaluate different mechanism, slices were also treated with TTX (1 μM), cytochalasin B (25 μM), high potassium medium (30 mM KCl), fluorocitrate (100 μM) and glucose (10, 1, 0.1 and 0 mM) in the presence, or not, of 1 mM STZ.

2.5. Surgical procedure

STZ was ICV infused, based on previous studies (Rodrigues et al., 2009; Biasibetti et al., 2017). Briefly, on the day of the surgery, animals were anesthetized with ketamine/xylazine (75 and 10 mg/kg, respectively, i.p.) and placed in a stereotaxic apparatus. A midline sagittal incision was made in the scalp. Burr holes were drilled in the skull on both sides over the lateral ventricles. The lateral ventricles were accessed using the following coordinates: 0.9 mm posterior to bregma; 1.5 mm lateral to sagittal suture; 3.6 mm beneath the surface of the brain. Rats received a single bilateral infusion of 5 μL STZ (3 mg/kg) or vehicle (Hank's balanced salt solution − HBSS −containing in mM: 137 NaCl; 0.63 Na_2HPO_4; 4.17 $NaHCO_3$; 5.36 KCl; 0.44 KH_2PO_4; 1.26 $CaCl_2$; 0.41 $MgSO_4$; 0.49 $MgCl_2$ and 10 glucose, in pH 7.4) using a Hamilton syringe. The infusion of 5μL/ventricle was carefully performed at a rate of 1 μL/min. After the surgical procedure, rats were placed on a heating pad to maintain body temperature at 37.5 ± 0.5 °C and were kept there until recovery from anesthesia. The animals were submitted to biochemical analysis at 48 h after STZ injection.

2.6. ELISA for S100B and GFAP

S100B content in the hippocampus and in the incubation medium of slices were determined by ELISA, as described previously (Leite et al., 2008). Briefly, 50 μL of sample plus 50 μL of Tris buffer were incubated for 2 h on a microtiter plate, previously coated with anti-S100B monoclonal antibody (SH-B1, from Sigma). Anti-S100 polyclonal antibody (from DAKO) was incubated for 30 min and then peroxidase-conjugated anti-rabbit antibody was added for a further 30 min. The color reaction with o-phenylenediamine was measured at 492 nm. The standard S100B curve ranged from 0.002 to 1 ng/mL. ELISA for GFAP in the hippocampal slice was carried out by coating the microtiter plate with 100 μL samples overnight at 4 °C. Incubation with a rabbit polyclonal anti-GFAP for 2 h was followed by incubation with a secondary antibody conjugated with peroxidase for 1 h, at room temperature; the standard GFAP curve ranged from 0.1 to 10 ng/mL (Tramontina et al.,

2007).

2.7. ELISA for BDNF

BDNF protein was assessed using the ChemiKine BDNF Sandwich ELISA kit (Millipore, USA), according to the manufacturer's recommendations. Briefly, the slices of hippocampus were individually homogenized in buffer containing 100 mM Tris-HCl (pH 7.0), containing 2% bovine serum albumin (BSA), 1 M NaCl, 4 mM EDTA·Na_2, 2% Triton X-100, 0.1% sodium azide, and a protease inhibitor cocktail (Sigma). Samples were centrifuged for 30 min at 14 000 × *g*. The hippocampus was homogenized and the slice incubation medium was incubated on a 96-well microplate previously coated with anti-BDNF monoclonal antibody. After blocking, plates were incubated with biotinylated mouse anti-BDNF monoclonal antibody for 3 h and streptavidin-HRP conjugate solution for 1 h. The color reaction with the 3,3′,5,5′-tetramethylbenzidine substrate was then quantified with a plate reader at 450 nm. The standard BDNF curve ranged from 7.8 to 500 pg/mL.

2.8. Glucose uptake assay

Glucose uptake was performed as previously described (Pellerin and Magistretti, 1994), with some modifications. Briefly, hippocampal slices were incubated at 35 °C in a Hank's balanced salt solution (HBSS). The assay was started by the addition of 0.1 μCi/well D-[3-^{3}H] deoxyglucose. The incubation was stopped after 30 min by removing the medium and rinsing the slices twice with ice-cold HBSS. The slices were then lysed in a 0.5 M NaOH solution. Radioactivity was measured using a scintillation counter. Glucose uptake was calculated by subtracting the nonspecific uptake, obtained by the glucose transporter inhibitor, cytochalasin B (25 μM), from the total uptake. Results were expressed as nmol/mg protein/min.

2.9. Western blot analysis

Proteins of sample were homogenized in sample buffer (62.5 mM Tris–HCl, pH 6.8, 10% (v/v) glycerol, 2% (w/v) SDS, 5% (w/v) β-mercaptoethanol and 0.002% bromphenol blue) and separated by SDS-PAGE on 10% (w/v) acrylamide gel and electro transferred onto nitrocellulose membranes. Membranes were incubated in TBS-T (20 mmol/L Tris–HCl, pH 7.5, 137 mmol/L NaCl, 0.05% (v/v) Tween 20) containing 5% (w/v) bovine serum albumin (BSA) for 1 h at room temperature. Subsequently, the membranes were incubated overnight with the appropriate primary antibody BDNF (dilution 1:1000) (Santa Cruz Biotechnology), and β-actin (dilution 1:5000) (Sigma Aldrich), rinsed with TBS-T, and exposed to horseradish peroxidase-linked anti-IgG antibodies for 2 h at room temperature. Chemiluminescent bands were detected using Image Quant LAS4000 GE Healthcare, and densitometry analyses were performed using Image-J software. The results were expressed as a percentage of the control.

2.10. Immunofluorescence

Protocol was performed accordingly (Biasibetti et al., 2017). Briefly, rats were anesthetized using ketamine/xylazine and were perfused through the left cardiac ventricle with 200 mL of saline solution, followed by 200 mL of 4% paraformaldehyde in 0.1 M phosphate buffer, pH 7.4. The brains were removed and left for post-fixation in the same fixative solution at 4 °C for 2 h. After this, the material was cryoprotected by immersing the brain in 15% and 30% sucrose in phosphate buffer at 4 °C. The brains were sectioned (40 μm) on a cryostat (Leitz) and incubated with polyclonal anti-GFAP from rabbit, diluted 1:500 in 2% BSA in PBS-Triton X-100 0.4%, for 48 h at 4 °C. After washing several times, tissue sections were incubated in secondary anti-rabbit IgG Alexa Fluor 586 (A11011), diluted 1:500 in PBS, at room temperature for 1 h. Afterwards, the sections were mounted on slides with Fluor Save® and covered with coverslips. Images were viewed with an Olympus confocal microscope and transferred to a computer with digital camera and Fluoviewer 3.1 FV1000 software.

2.11. Lactate dehydrogenase assay for membrane integrity

The lactate dehydrogenase (LDH) assay was conducted in 150 μL of extracellular medium using a commercial kinetic UV assay from Bioclin (Brazil), according to the manufacturer's instructions. Results are expressed as percentages of the control value.

2.12. MTT reduction assay for cell viability

Slices were treated with 0.5 mg/mL of MTT for 30 min at 30 °C. The MTT formazan was dissolved in DMSO. Absorbance values were measured at 560 and 650 nm. Results are expressed as percentages of the control value (Hansen et al., 1989).

2.13. Protein determination

Protein content was measured by Lowry's method with some modifications, using bovine serum albumin as the standard (Peterson, 1977).

2.14. Statistical analysis

For brain hippocampal slices, data are presented as mean ± S.E.M. Each experiment was performed in triplicate (i.e., 3 slices from each rat) in at least six independent experiments (i.e., 6 rats). The data were subjected to one-way analysis of variance (ANOVA), followed by the Tukey's test. Correlations were analysed by Pearson correlation coefficient. For the *in vivo* STZ model, data are presented as mean ± S.E.M. and statistically evaluated by Student's t-test. Values of $P < 0.05$ were considered significant. All analyses were performed using the Graphpad Prism software version 6 (La Jolla, CA, USA).

3. Ethics statement

All animal experiments were carried out in accordance with the National Institutes of Health Guide for the Care and Use of Laboratory Animals and were approved by the Federal University of Rio Grande do Sul Animal Care and Use Committee (process number 28035).

4. Results

4.1. STZ decreases S100B secretion but increases BDNF in hippocampal slices

We evaluated three concentrations of STZ (0.1, 1 and 10 mM), based on cell culture studies (Plaschke and Kopitz, 2015). In Fig. 1A ($p < 0.0001$ and $F_{(3,16)} = 15.53$), we show that STZ exposure decreased S100B secretion, in a concentration-dependent manner. On the other hand, BDNF secretion was induced by STZ at 1 mM (Fig. 1B) ($p = 0.0028$ and $F_{(3,15)} = 7.440$). We have used the term “secretion” because we measured S100B and BDNF proteins in the incubation medium, and cell integrity in hippocampal slices was confirmed by unchanged levels of LDH (Fig. 1C) ($p = 0.9858$ and $F_{(3,26)} = 0.04736$). Moreover, the viability of these preparations was examined by an MTT reduction assay (Fig. 1D) ($p = 0.5582$ and $F_{(3,16)} = 0.7133$). In all experiments, both MTT and LDH were evaluated and statistical differences were not observed (data not shown).

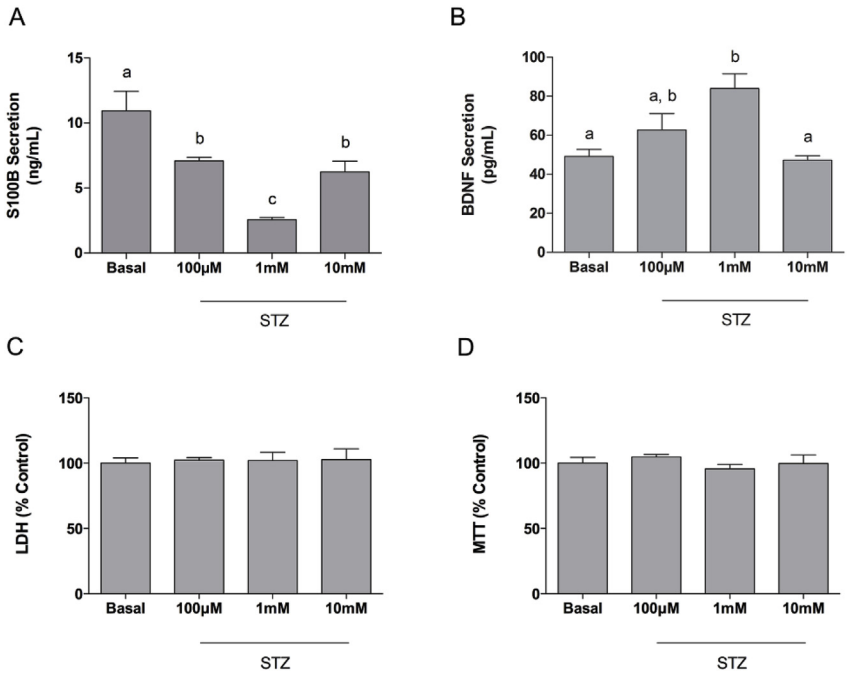

Fig. 1. Effect of STZ on S100B and BDNF secretion in acute hippocampal slices. A, Fresh hippocampal slices were incubated in the presence of STZ, at indicated concentrations, and S100B secretion was measured by ELISA 1 h afterwards. B, Fresh hippocampal slices were incubated in the presence of STZ for 1 h and the BDNF concentration in the incubation medium was measured by ELISA. C, Evaluation of cell integrity of hippocampal slices during STZ exposure was measured by LDH activity in the incubation medium. D, MTT reduction assay was used for evaluation of cell viability in hippocampal slices. Data are shown as absolute values (A and B) or percentage means ± SE of 6 independent experiments performed in triplicate. Letters indicate different statistical groups (one-way ANOVA followed by Tukey's test).

4.2. STZ exposure causes impairment in glucose uptake in hippocampal slices

Since STZ affects glucose flux we measured its direct effect on glucose uptake. In fact, STZ decreased glucose uptake in a concentration-dependent manner (Fig. 2A) ($p < 0.0001$ and $F_{(3,16)} = 59.32$). In another set of experiments, we measured glucose uptake and S100B secretion, or BDNF secretion, in hippocampal slices exposed to different concentrations of STZ. A positive correlation between the STZ-induced decrease in glucose uptake and the decrease in S100B secretion was observed (Fig. 2B, $r = 0.7872$, $p < 0.0001$). However, no correlation was observed between the decrease in glucose uptake and the increase in BDNF secretion in hippocampal slices exposed to STZ (Fig. 2C, $r = -0.06020$, $p = 0.8066$).

4.3. Glucose levels and glucose metabolism differentially modulate S100B and BDNF secretion

We investigated the effect of different glucose concentrations in the incubation medium on S100B (Fig. 3A) ($p = 0.8902$ and $F_{(3,23)} = 0.2068$) and BDNF (Fig. 3B) ($p = 0.0486$ and $F_{(3,23)} = 3.058$) in acute hippocampal slices. Note that 10 mM glucose was the basal concentration used in our experiments. Lower levels of glucose (1 and 0.1 mM) or even the absence of glucose in the incubation medium do not alter S100B secretion. However, an increase in BDNF secretion was observed when hippocampal slices were incubated with lower levels of glucose. In order to clarify the effect of glucose, we incubated hippocampal slices with cytochalasin B, an inhibitor of glucose transport, and fluorocitrate, a preferential astrocytes metabolic inhibitor. S100B secretion was not affected by cytochalasin B, but was dramatically inhibited by flurocitrate (Fig. 3C) ($p < 0.0001$ and $F_{(2,12)} = 143.0$). On the other hand, cytochalasin B and fluorocitrate stimulated BDNF secretion (Fig. 3D) ($p = 0.0041$ and $F_{(2,21)} = 7.223$).

4.4. The effects of STZ on S100B and BDNF secretion are cell-specific

In order to confirm the cell sources of S100B and BDNF, as well as the possible alterations in membrane depolarization induced by STZ, we incubated hippocampal slices in the presence of high potassium medium (high K^+) and tetrodotoxin (TTX), an inhibitor of voltage-regulated Na^+ channels. High K^+ induced a decrease in S100B secretion, while TTX had no effect *per se* on S100B secretion (Fig. 4A) ($p = 0.0011$ and $F_{(3,16)} = 8.891$). However, TTX partially restores the STZ-induced reduction in S100B secretion induced by high K^+. Moreover, the decrease in S100B secretion caused by STZ (at 1 mM) was not prevented by the presence of TTX (Fig. 4B) ($p = 0.0005$ and $F_{(2,12)} = 15.24$). BDNF secretion was stimulated in high K^+ and TTX was able to partially block this stimulation (Fig. 4C) ($p = 0.0149$ and $F_{(3,42)} = 3.917$). However, TTX tended to diminish STZ-stimulated BDNF secretion (Fig. 4D) ($p = 0.0027$ and $F_{(2,31)} = 7.229$).

4.5. Intracerebroventricular STZ reduces hippocampal BDNF content but not S100B

In order to evaluate the acute *in vivo* toxicity of STZ, we infused this compound ICV (3 mg/kg, bilaterally) and determined the content of BDNF and S100B in the hippocampus 48 h later. The hippocampal BDNF content was reduced when analysed by ELISA (Fig. 5A, $p = 0.0396$), as well as when observed by Western blotting (Fig. 5B, $p = 0.0329$). On the other hand, the hippocampal content of S100B was unchanged (Fig. 5C, $p = 0.7104$). However, the astroglial reactivity indicated GFAP increment (Fig. 5D, $p = 0.0391$). Immunohistochemistry analysis for GFAP confirmed the hippocampal glial commitment to STZ exposure (Fig. 5, panels F and G).

5. Discussion

The present study provides data that help to elucidate the early alterations and acute mechanisms of STZ toxicity and disease mechanisms in the brain tissue. Most studies have characterized cell death markers even several weeks after ICV STZ, identifying long-term changes rather than a direct toxic effect of this compound (Saxena et al., 2011; Rai et al., 2014). The STZ-induced model of AD is well established but the direct and acute effects of this compound on nervous tissue are poorly understood. In fact, only a few studies have looked at the acute effects of STZ on brain tissue. Herein, we investigated STZ toxicity and glucose metabolism dysfunction in the hippocampus by looking at its direct effects on *ex vivo* preparations, evaluating two well-characterized markers of brain injury, BDNF and S100B. Additionally, early hippocampal alterations in these markers

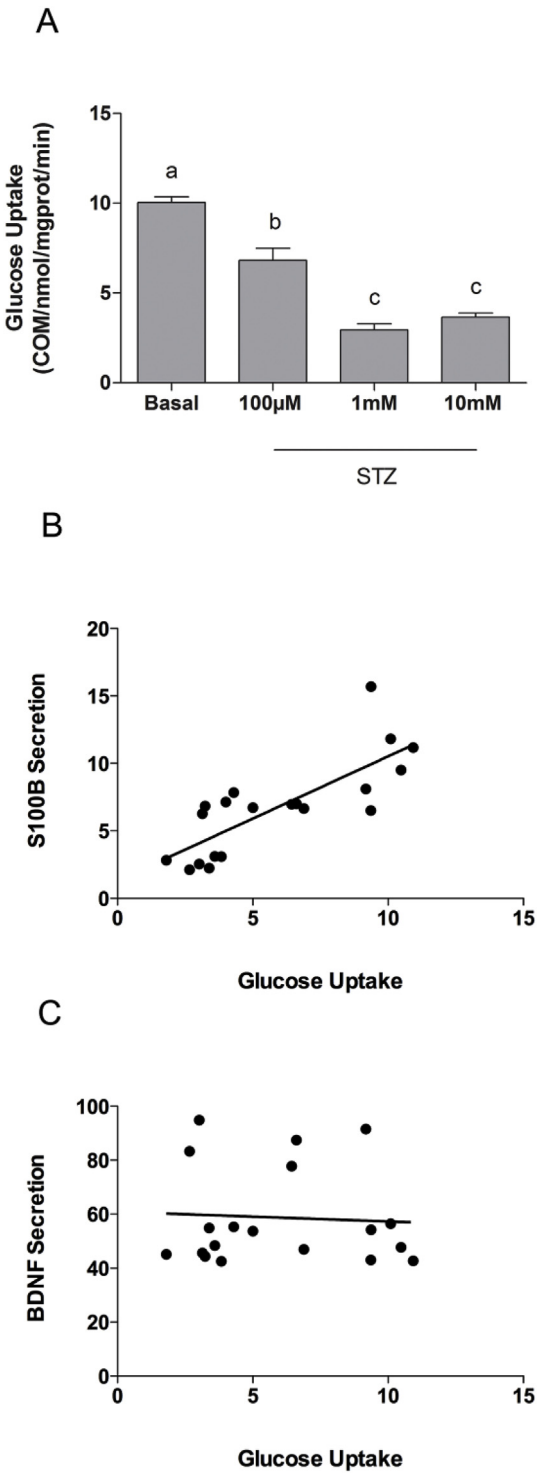

Fig. 2. Effect of STZ on glucose uptake in hippocampal slices. A, Fresh hippocampal slices were incubated in the presence of STZ for 1 h, at indicated concentrations, and glucose uptake was measured in the last 30 min by addition of [^{3}H]-deoxy-glucose. Data are shown are means ± SE of 6 independent experiments (six animals) performed in triplicate (three slices from each animal, one slice/well). Letters indicate different statistical groups (one-way ANOVA followed by Tukey's test). In another set of experiments experiments, we searched determined the correlation between glucose uptake and S100B secretion (in B) or glucose uptake and BDNF secretion (in B) in hippocampal slices exposed to STZ, as analysed by Pearson correlation coefficient, assuming $p < 0.05$.

were also determined at 48 h after STZ exposure *in vivo*.

STZ impairs the glucose metabolism in many cell types and is apparently influenced by the presence of GLUT2 (Szkudelski 2001, 2012). N2A neuronal cultures and C6 glioma cells exposed to STZ (from 0.01 to 1 mM) for 48 h exhibited decreases in glucose uptake, accompanied by lower ATP levels and decreased glucose transporter expression (Biswas et al., 2016; Biswas et al., 2017). The decrease in extracellular S100B has been related to glucose metabolism in hippocampal slices and C6 glioma cells (Wartchow et al., 2016) and our observation of a decrease in glucose uptake reinforces a possible association. Moreover, a positive correlation was observed between the decrease in S100B and the decrease in glucose uptake induced by STZ. In the STZ model of AD, both hippocampal glucose uptake and decreased cerebrospinal fluid S100B have been reported (Rodrigues et al., 2009; Biasibetti et al., 2013). Although the mechanism remains unclear, the STZ-induced interference in glucose metabolism is associated with reduced extracellular levels of S100B.

On the other hand, STZ (at 1 mM, but not at 10 mM) stimulated BDNF release in acute hippocampal slices; this effect was not attributable to "leaking" of BDNF, once no changes were observed in cell viability (measured by MTT reduction assay) or cell integrity (measured by LDH release) following STZ incubation at this concentration. BDNF is also released by neurons to increase glucose utilization (see Marosi and Mattson, 2014 for a review), therefore, the increment observed may suggest a neuronal response to glucose metabolism impairment. However, no direct correlation was observed between the decrease in glucose uptake and BDNF secretion from hippocampal slices.

In order to investigate whether the opposing changes in S100B and BDNF secretion are related to glucose metabolism, we evaluated whether this secretion is affected by extracellular levels of glucose or glucose uptake or glucose metabolism. S100B secretion by astrocytes was not affected by levels of glucose (from 0 to 10 mM, which is the basal concentration in our conditions). However, BDNF secretion was clearly higher when hippocampal slices were incubated in a medium without glucose. Moreover, when cytochalasin B, a non-specific inhibitor of glucose transport, was added to the incubation medium, BDNF secretion was strongly stimulated, but S100B secretion was not. A summary of our results is represented in Fig. 6. More dramatic and opposing effects were observed when slices were incubated with fluorocitrate, an inhibitor of aconitase, which is mostly uptaken by glial cells. Fluorocitrate stimulated BDNF secretion and strongly reduced S100B secretion via an, as yet, undefined mechanism, although it is possible that glucose or its metabolites, such as lactate or methylglyoxal, may be involved in this effect (see Fig. 6). Both glucose-derived products are metabolic substrates and additionally act on membrane receptors (Distler and Palmer, 2012; Barros et al., 2013; Gonçalves et al., 2018), which in turn, could modulate the secretion of S100B in astrocytes and BDNF in neurons. While the mechanisms involved in glucose flow and the opposing alterations in BDNF and S100B secretion are unknown, these effects are quite clear.

At this point in the study, we assumed that S100B and BDNF are secreted by astrocytes and neurons, respectively, by opposing and independent mechanisms. Our next step was to investigate whether S100B was, in fact, released from astrocytes and BDNF from neurons in our preparations. For this, we used TTX, a blocker of Na^+ channels (almost absent in glial cells) and a high K^+ -medium that is able to depolarize neurons (and therefore stimulate BDNF secretion) and negatively modulate S100B secretion in astrocytes (Nardin et al., 2009). In fact, the high K^+ -medium stimulated BDNF secretion in hippocampal slices and this effect was blocked by co-incubation with TTX (see Fig. 6). This confirms the neuronal origin of extracellular BDNF. Astrocytes are also able to express and secrete BDNF in some injury conditions (Bergami et al., 2008), but possibly not in this STZ-induced acute damage model. On the other hand, high K^+ -medium caused a decrease in S100B secretion and this was partially blocked by TTX, suggesting that high K^+-reduced S100B secretion, involves, in part,

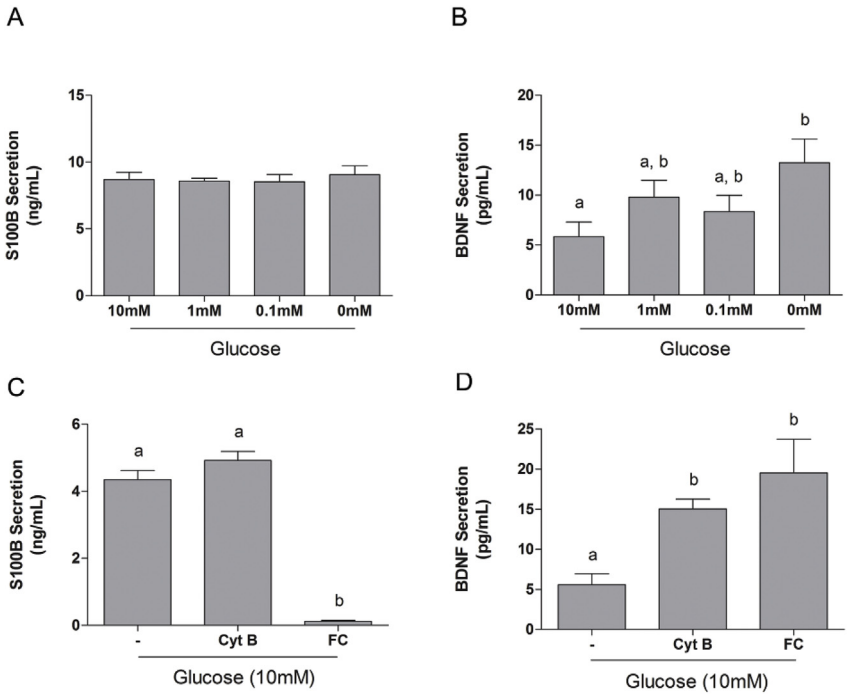

Fig. 3. The effect of glucose levels and glucose metabolism on S100B and BDNF secretion in acute hippocampal slices. Acute hippocampal slices were incubated for 1 h in media with different concentrations of glucose, as indicated in the Figure, and S100B secretion (in A) and BDNF secretion (in B) were measured. Hippocampal slices were incubated with cytochalasin B (Cyt B) at 25 μM, an inhibitor of glucose transport, or fluorocitrate (FC) at 100 μM, a glia-specific metabolic inhibitor, to evaluate and S100B secretion (Fig. 3C) and BDNF secretion (Fig. 3D) were evaluated. Data are means ± SE of 6 independent experiments performed in triplicate. Letters indicate different statistical groups (one-way ANOVA followed by Tukey's test).

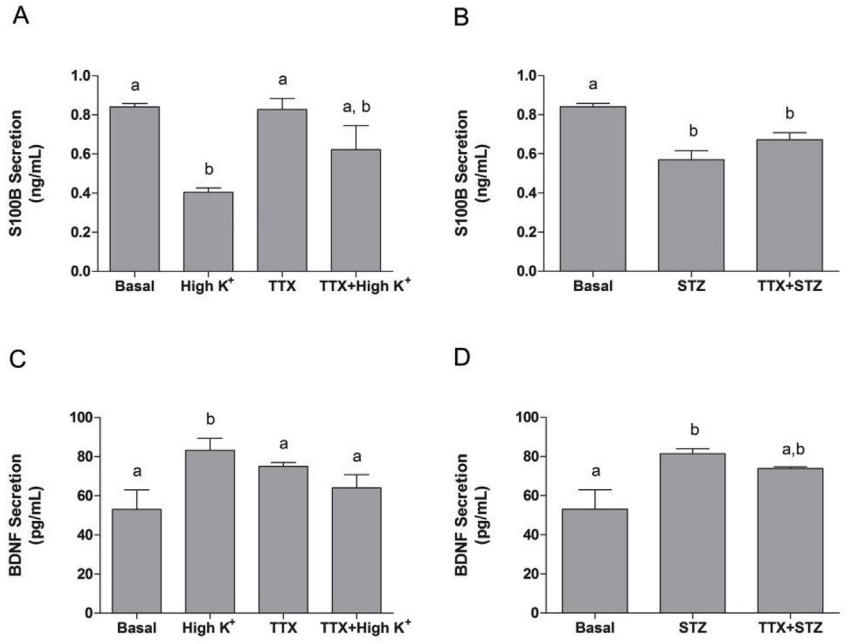

Fig. 4. The effect of tetrodotoxin on STZ -induced changes in S100B and BDNF. A, S100B secretion was evaluated in hippocampal slices incubated in basal and high potassium medium conditions (30 mM KCl) and in the presence or not of TTX (1 μM). B, S100B secretion in the presence of STZ (at 1 mM) and TTX C, BDNF secretion was evaluated in hippocampal slices incubated in the basal and high potassium medium and in the presence or not of TTX. D, BDNF secretion in the presence of STZ (at 1 mM) and TTX (at 1 μM). Data are means ± SE of 6 independent experiments performed in triplicate. Letters indicate different statistical groups (one-way ANOVA followed by Tukey's test).

some neuronal pathways. However, STZ-reduced S100B secretion was not affected by TTX. The BDNF secretion induced by STZ was partially inhibited by TTX, reinforcing the idea that BDNF is secreted, in part, independently of neuronal depolarization.

Abnormalities in glucose metabolism in the hippocampus, in addition to neurodegenerative diseases, are observed in psychiatric disorders and schizophrenia in their early stages (Schöll et al., 2014), and perhaps changes in the secretion of S100B and/or BDNF in this region of the brain are linked to these abnormalities (Kalia and Costa E Silva, 2015; Dorofeikova et al., 2018). Type 2 DM is a frequent comorbidity in bipolar disorder, and the hippocampus is strongly affected (Hajek et al., 2014)et al., 2014). In fact, a postmortem study in the hippocampus showed a decrease of S100B-immunopositive astrocytes and oligodendrocytes in CA1 in major depression disorder and bipolar disorder (Gos et al., 2013). Accordingly, we found that fluoxetine stimulated the secretion of S100B into slices of rat hippocampus (Tramontina et al., 2008).

In addition, impairment of glucose metabolism is observed in schizophrenic individuals and antipsychotic medication may contribute to this alteration (Steiner et al., 2014). Hippocampal slices exposed to apomorphine, which mimic dopaminergic hyperactivation, have a reduced secretion of S100B, which is prevented by haloperidol and risperidone (Nardin et al., 2011). On the other hand, these antipsychotics were also capable of preventing the secretion of S100B induced by IL6 (de Souza et al., 2013).

In other experiments, anesthetized rats received an ICV administration of STZ and both markers, BDNF and S100B, were analysed in hippocampal tissue. No changes were observed in the hippocampal

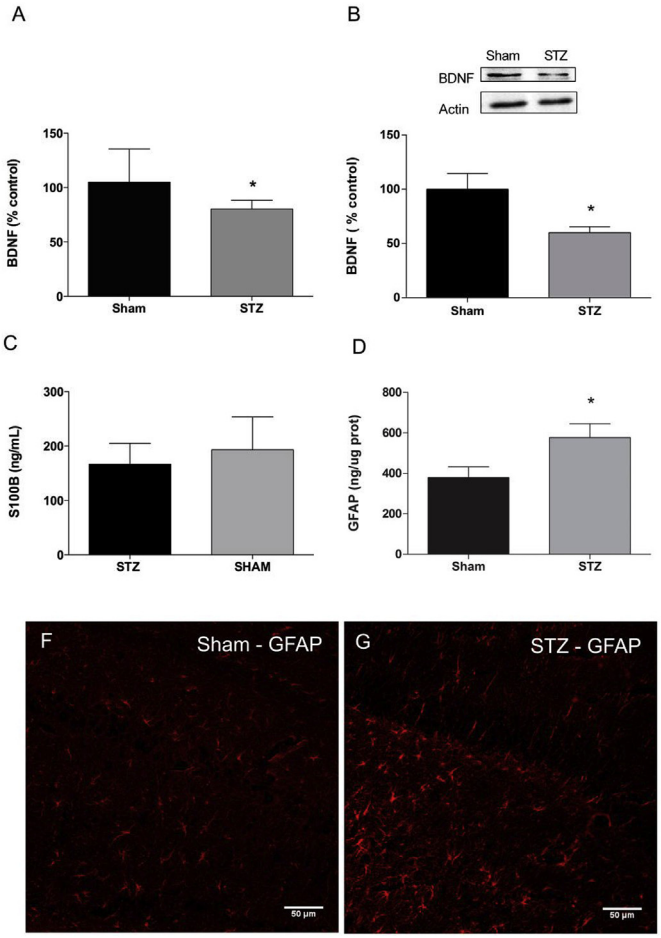

Fig. 5. The effect of ICV administration of STZ on S100B, GFAP and BDNF content. Anesthetised rats received ICV STZ (3 mg/kg) or vehicle (Sham) and hippocampal tissue was collected 48 h afterwards. S100B (panel C) and GFAP (panel D) contents were analysed by ELISA. BDNF content was measured by ELISA (panel A) and by Western blotting (panel B). Panels F and G show a representative image for GFAP immunoreactivity. Values are means ± SE. * Statistical significance (N = 8–9, Student's t-test, $p < 0.05$).

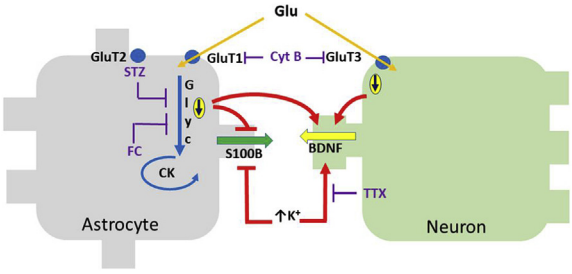

Fig. 6. Schematic representation of S100B and BDNF secretion in hippocampal slices. Glucose enters mainly through GLUT1 and GLUT3 transporters in astrocytes and neurons, respectively. STZ, which possibly enters via GLUT2, causes a decrease in secretion of S100B, but an increase in neuronal secretion of BDNF. Fluorocitrate (FC), which inhibits glial aconitase, does the same. BDNF secretion was sensitive to extracellular levels and glucose transport (inhibited by cytochalasin B, Cyt B). Cell origin of BDNF and S100B was investigated in a high-potassium medium (↑K^+), containing or not tetrodotoxin (TTX) to block voltage-dependent sodium channels. Glyc = glycolysis; CK = cycle of Krebs.

content of S100B, compared to sham rats 48 h afterwards. However, the increase in GFAP suggests astroglial commitment, which was confirmed by immunocytochemistry. Accordingly, rapid changes have been reported in GFAP (and GLUT-2) immunoreactivity at 1 and 24 h after ICV STZ infusion in different mouse brain regions, including the hippocampus (Knezovic et al., 2017). A recent study from our laboratory showed increased GFAP in the hippocampus at one week after STZ infusion (Dos Santos, Vizuete et al., 2018), confirming the long-term STZ-induced astrogliosis observed by other authors (Javed et al., 2012; Mishra et al., 2018). This direct and acute effect on GFAP was also observed in C6 glioma cells exposed to STZ for 24 h (Rajasekar et al., 2014).

Differently from observations with S100B, we found that hippocampal BDNF was reduced at 48 h after ICV STZ administration, as measured by ELISA or Western blotting. Our results are also in agreement with the fast hippocampal BDNF decrement observed at one and 24 h after ICV STZ infusion (Souza et al., 2017). In C6 glioma cells exposed to STZ, BDNF expression was also reduced at 48 h (Rajasekar et al., 2016), as occurred in RIN5F cells (an insulin-secreting rat pancreatic β cell line) (Bathina et al., 2017). Moreover, other studies found a decrease in BDNF in whole brain and hippocampal tissue at 3 weeks after ICV STZ administration (Sharma and Gupta, 2002; Sharma and Taliyan, 2015; Rajasekar et al., 2017).

Taken together, these data suggest that acute STZ does not affect the hippocampal S100B content, but reduces its secretion and concomitantly increases BDNF secretion. Moreover, our data indicate the usefulness of this model in pre-clinical studies to investigate S100B and BDNF. It is also important to note that most studies that correlate glucose metabolism and BDNF refer to protein expression rather than secretion, as we have measured here. However, we are aware that our *in vitro* results (concerning protein secretion) cannot be compared directly with *in vivo* results (concerning protein turnover). Under *in vitro* conditions, we can observe the secretion of S100B and BDNF in response to STZ, where changes in the expression of these proteins in the hippocampal slice is likely very small. For a direct comparison between *in vitro* and *in vivo* conditions, it would appear to be more appropriate to measure hippocampal secretion *ex vivo* at 1 h after ICV STZ administration. However, due to the methodological approach used for slice preparations (that takes 2 h), we can determine secretion of S100B and BDNF at 3 h after STZ *and* in anesthetized rats that, in turn, could affect protein secretion (Vicente et al., 2007). Independently of these limitations, these *in vitro* and *in vivo* results are important for understanding the response to acute exposure to STZ.

6. Conclusions

In summary, our results clearly show that STZ acutely affects the secretion of S100B (decrease) and BDNF (increase) from astrocytes and neurons, respectively. Using fresh hippocampal slices, in which these cells are structurally and functionally preserved, it is possible to observe a complex metabolic relationship. The impairment of glucose metabolism by STZ directly and indirectly affected the secretion of the S100B and BDNF proteins. Our results indicate that BDNF and S100B are useful and sensitive markers of acute energetic metabolic changes induced by STZ and in other brain injury conditions.

Conflicts of interest

The authors declare no competing financial interest.

Acknowledgments

Funding agencies CAPES, CNPq, FAPERGS and INCT for Excitotoxicity and Neuroprotection.

References

Baranowska-Bosiacka, I., et al., 2013. Perinatal exposure to lead induces morphological, ultrastructural and molecular alterations in the hippocampus. Toxicology 303, 187–200.

Barros, L.F., et al., 2013. Small is fast: astrocytic glucose and lactate metabolism at cellular resolution. Front. Cell. Neurosci. 7, 27.
Bathina, S., Das, U.N., 2018. Dysregulation of PI3K-Akt-mTOR pathway in brain of streptozotocin-induced type 2 diabetes mellitus in Wistar rats. Lipids Health Dis. 17 (1), 168.
Bathina, S., et al., 2017. Streptozotocin produces oxidative stress, inflammation and decreases BDNF concentrations to induce apoptosis of RIN5F cells and type 2 diabetes mellitus in Wistar rats. Biochem. Biophys. Res. Commun. 486 (2), 406–413.
Bennett, R.A., Pegg, A.E., 1981. Alkylation of DNA in rat tissues following administration of streptozotocin. Cancer Res. 41 (7), 2786–2790.
Bergami, M., et al., 2008. Uptake and recycling of pro-BDNF for transmitter-induced secretion by cortical astrocytes. J. Cell Biol. 183 (2), 213–221.
Biasibetti, R., et al., 2017. Hippocampal changes in STZ-model of Alzheimer's disease are dependent on sex. Behav. Brain Res. 316, 205–214.
Biasibetti, R., et al., 2013. Green tea (-)epigallocatechin-3-gallate reverses oxidative stress and reduces acetylcholinesterase activity in a streptozotocin-induced model of dementia. Behav. Brain Res. 236 (1), 186–193.
Biswas, J., et al., 2016. Streptozotocin induced neurotoxicity involves Alzheimer's related pathological markers: a study on N2A cells. Mol. Neurobiol. 53 (5), 2794–2806.
Biswas, J., et al., 2017. Streptozotocin alters glucose transport, connexin expression and endoplasmic reticulum functions in neurons and astrocytes. Neuroscience 356, 151–166.
Brouwers, B., et al., 2013. Phlorizin pretreatment reduces acute renal toxicity in a mouse model for diabetic nephropathy. J. Biol. Chem. 288 (38), 27200–27207.
Chen, Z., Zhong, C., 2013. Decoding Alzheimer's disease from perturbed cerebral glucose metabolism: implications for diagnostic and therapeutic strategies. Prog. Neurobiol. 108, 21–43.
de Souza, D.F., et al., 2013. Interleukin-6-induced S100B secretion is inhibited by haloperidol and risperidone. Prog. Neuro-Psychopharmacol. Biol. Psychiatry 43, 14–22.
Distler, M.G., Palmer, A.A., 2012. Role of Glyoxalase 1 (Glo1) and methylglyoxal (MG) in behavior: recent advances and mechanistic insights. Front. Genet. 3, 250.
Donato, R., 2007. RAGE: a single receptor for several ligands and different cellular responses: the case of certain S100 proteins. Curr. Mol. Med. 7 (8), 711–724.
Dorofeikova, M., et al., 2018. Cognitive deficit in patients with paranoid schizophrenia: its clinical and laboratory correlates. Psychiatr. Res. 262, 542–548.
Dos Santos, J.P.A., et al., 2018. Early and persistent O-GlcNAc protein modification in the streptozotocin model of Alzheimer's disease. J. Alzheimer's Dis. 61 (1), 237–249.
Eizirik, D.L., et al., 1993. Genotoxic agents increase expression of growth arrest and DNA damage–inducible genes gadd 153 and gadd 45 in rat pancreatic islets. Diabetes 42 (5), 738–745.
Fernandes, B.S., et al., 2014. Decreased peripheral brain-derived neurotrophic factor levels are a biomarker of disease activity in major psychiatric disorders: a comparative meta-analysis. Mol. Psychiatr. 19 (7), 750–751.
Flores-Gómez, A.A., et al., 2019. Consequences of diabetes mellitus on neuronal connectivity in limbic regions. Synapse 73 (3), e22082.
Frölich, L., et al., 1998. Brain insulin and insulin receptors in aging and sporadic Alzheimer's disease. J. Neural Transm. 105 (4–5), 423–438.
Galland, F., et al., 2017. Hyperammonemia compromises glutamate metabolism and reduces BDNF in the rat hippocampus. Neurotoxicology 62, 46–55.
Gonçalves, C.A., et al., 2008. Biological and methodological features of the measurement of S100B, a putative marker of brain injury. Clin. Biochem. 41 (10–11), 755–763.
Gonçalves, C.A., et al., 2018. Glycolysis-derived compounds from astrocytes that modulate synaptic communication. Front. Neurosci. 12, 1035.
Gos, T., et al., 2013. S100B-immunopositive astrocytes and oligodendrocytes in the hippocampus are differentially afflicted in unipolar and bipolar depression: a post-mortem study. J. Psychiatr. Res. 47 (11), 1694–1699.
Hajek, T., et al., 2014. Insulin resistance, diabetes mellitus, and brain structure in bipolar disorders. Neuropsychopharmacology 39 (12), 2910–2918.
Hansen, M.B., et al., 1989. Re-examination and further development of a precise and rapid dye method for measuring cell growth/cell kill. J. Immunol. Methods 119 (2), 203–210.
Harb, G., et al., 2007. Acute exposure to streptozotocin but not human proinflammatory cytokines impairs neonatal porcine islet insulin secretion in vitro but not in vivo. Xenotransplantation 14 (6), 580–590.
Hoyer, S., et al., 1994. Desensitization of brain insulin receptor. Effect on glucose/energy and related metabolism. J. Neural Transm. Suppl. 44, 259–268.
Javed, H., et al., 2012. Rutin prevents cognitive impairments by ameliorating oxidative stress and neuroinflammation in rat model of sporadic dementia of Alzheimer type. Neuroscience 210, 340–352.
Ju, T., et al., 2016. Streptozotocin inhibits electrophysiological determinants of excitatory and inhibitory synaptic transmission in CA1 pyramidal neurons of rat hippocampal slices: reduction of these effects by edaravone. Cell. Physiol. Biochem. 40 (6), 1274–1288.
Kalia, M., Costa E Silva, J., 2015. Biomarkers of psychiatric diseases: current status and future prospects. Metabolism 64 (3 Suppl. 1), S11–S15.
Katakam, A.K., et al., 2005. Streptozotocin (STZ) mediates acute upregulation of serum and pancreatic osteopontin (OPN): a novel islet-protective effect of OPN through inhibition of STZ-induced nitric oxide production. J. Endocrinol. 187 (2), 237–247.
Kimura, A., et al., 2016. Neuroprotection, growth factors and BDNF-TrkB signalling in retinal degeneration. Int. J. Mol. Sci. 17 (9).
Knezovic, A., et al., 2017. Rat brain glucose transporter-2, insulin receptor and glial expression are acute targets of intracerebroventricular streptozotocin: risk factors for sporadic Alzheimer's disease? J. Neural Transm. 124 (6), 695–708.
Kowiański, P., Lietzau, G., Czuba, E., Waśkow, M., Steliga, A., Moryś, J., 2018 Apr. BDNF: a key factor with multipotent impact on brain signaling and synaptic plasticity. Cell. Mol. Neurobiol. 38 (3), 579–593. https://doi.org/10.1007/s10571-017-0510-4. Epub 2017 Jun 16.
Kraska, A., et al., 2012. In vivo cross-sectional characterization of cerebral alterations induced by intracerebroventricular administration of streptozotocin. PLoS One 7 (9), e46196.
Lannert, H., Hoyer, S., 1998. Intracerebroventricular administration of streptozotocin causes long-term diminutions in learning and memory abilities and in cerebral energy metabolism in adult rats. Behav. Neurosci. 112 (5), 1199–1208.
Leite, M.C., et al., 2008. A simple, sensitive and widely applicable ELISA for S100B: methodological features of the measurement of this glial protein. J. Neurosci. Methods 169 (1), 93–99.
Leite, M.C., et al., 2017. S100B secretion is mediated by Ca2+ from endoplasmic reticulum: a study using DMSO as a tool for intracellular Ca2+ mobilization. Glia 65 (S1), E558.
Marosi, K., Mattson, M.P., 2014. BDNF mediates adaptive brain and body responses to energetic challenges. Trends Endocrinol. Metabol. 25 (2), 89–98.
Mishra, S.K., et al., 2018. Intracerebroventricular streptozotocin impairs adult neurogenesis and cognitive functions via regulating neuroinflammation and insulin signaling in adult rats. Neurochem. Int. 113, 56–68.
Nardin, P., et al., 2009. S100B secretion in acute brain slices: modulation by extracellular levels of Ca(2+) and K (+). Neurochem. Res. 34 (9), 1603–1611.
Nardin, P., et al., 2011. In vitro S100B secretion is reduced by apomorphine: effects of antipsychotics and antioxidants. Prog. Neuro-Psychopharmacol. Biol. Psychiatry 35 (5), 1291–1296.
Nardin, P., et al., 2016. Peripheral levels of AGEs and astrocyte alterations in the Hippocampus of STZ-diabetic rats. Neurochem. Res. 41 (8), 2006–2016.
Ohaeri, J.U., Akanji, A.O., 2011. Metabolic syndrome in severe mental disorders. Metab. Syndrome Relat. Disord. 9 (2), 91–98.
Okusaka, T., et al., 2015. Cytotoxic chemotherapy for pancreatic neuroendocrine tumors. J Hepatobiliary Pancreat Sci 22 (8), 628–633.
Pellerin, L., Magistretti, P.J., 1994. Glutamate uptake into astrocytes stimulates aerobic glycolysis: a mechanism coupling neuronal activity to glucose utilization. Proc. Natl. Acad. Sci. U. S. A. 91 (22), 10625–10629.
Peterson, G.L., 1977. A simplification of the protein assay method of Lowry et al. which is more generally applicable. Anal. Biochem. 83 (2), 346–356.
Plaschke, K., Kopitz, J., 2015. In vitro streptozotocin model for modeling Alzheimer-like changes: effect on amyloid precursor protein secretases and glycogen synthase kinase-3. J. Neural Transm. 122 (4), 551–557.
Rai, S., et al., 2014. Glial activation and post-synaptic neurotoxicity: the key events in Streptozotocin (ICV) induced memory impairment in rats. Pharmacol. Biochem. Behav. 117, 104–117.
Rajasekar, N., et al., 2014. Protection of streptozotocin induced insulin receptor dysfunction, neuroinflammation and amyloidogenesis in astrocytes by insulin. Neuropharmacology 86, 337–352.
Rajasekar, N., et al., 2016. Inhibitory effect of memantine on streptozotocin-induced insulin receptor dysfunction, neuroinflammation, amyloidogenesis, and neurotrophic factor decline in astrocytes. Mol. Neurobiol. 53 (10), 6730–6744.
Rajasekar, N., et al., 2017. Intranasal insulin improves cerebral blood flow, Nrf-2 expression and BDNF in STZ (ICV)-induced memory impaired rats. Life Sci. 173, 1–10.
Regenold, W.T., et al., 2002. Increased prevalence of type 2 diabetes mellitus among psychiatric inpatients with bipolar I affective and schizoaffective disorders independent of psychotropic drug use. J. Affect. Disord. 70 (1), 19–26.
Rodrigues, L., et al., 2009. Hippocampal alterations in rats submitted to streptozotocin-induced dementia model are prevented by aminoguanidine. J. Alzheimer's Dis. 17 (1), 193–202.
Rosa, E., et al., 2016. Tau downregulates BDNF expression in animal and cellular models of Alzheimer's disease. Neurobiol. Aging 48, 135–142.
Rosenberger, C., et al., 2008. Acute kidney injury in the diabetic rat: studies in the isolated perfused and intact kidney. Am. J. Nephrol. 28 (5), 831–839.
Salkovic-Petrisic, M., et al., 2013. What have we learned from the streptozotocin-induced animal model of sporadic Alzheimer's disease, about the therapeutic strategies in Alzheimer's research. J. Neural Transm. 120 (1), 233–252.
Saxena, G., et al., 2011. ICV STZ induced impairment in memory and neuronal mitochondrial function: a protective role of nicotinic receptor. Behav. Brain Res. 224 (1), 50–57.
Schöll, M., et al., 2014. Fluorodeoxyglucose PET in neurology and psychiatry. Pet. Clin. 9 (4), 371–390 (v).
Serra-Millàs, M., 2016. Are the changes in the peripheral brain-derived neurotrophic factor levels due to platelet activation? World J. Psychiatr. 6 (1), 84–101.
Sharma, M., Gupta, Y.K., 2002. Chronic treatment with trans resveratrol prevents intracerebroventricular streptozotocin induced cognitive impairment and oxidative stress in rats. Life Sci. 71 (21), 2489–2498.
Sharma, S., Taliyan, R., 2015. Synergistic effects of GSK-3β and HDAC inhibitors in intracerebroventricular streptozotocin-induced cognitive deficits in rats. Naunyn-Schmiedeberg's Arch. Pharmacol. 388 (3), 337–349.
Souza, L.C., Jesse, C.R., de Gomes, M.G., Del Fabbro, L., Goes, A.T.R., Donato, F., Boeira, S.P., 2017 Oct. Activation of brain indoleamine-2,3-dioxygenase contributes to depressive-like behavior induced by an intracerebroventricular injection of streptozotocin in mice. Neurochem. Res. 42 (10), 2982–2995. https://doi.org/10.1007/s11064-017-2329-2. Epub 2017 Jun 19.
Stanne, T.M., et al., 2016. Low circulating acute brain-derived neurotrophic factor levels are associated with poor long-term functional outcome after ischemic stroke. Stroke 47 (7), 1943–1945.
Steiner, J., et al., 2014. Immune system and glucose metabolism interaction in schizophrenia: a chicken-egg dilemma. Prog. Neuro-Psychopharmacol. Biol. Psychiatry 48, 287–294.
Szkudelski, T., 2001. The mechanism of alloxan and streptozotocin action in B cells of the

rat pancreas. Physiol. Res. 50 (6), 537–546.
Szkudelski, T., 2012. Streptozotocin-nicotinamide-induced diabetes in the rat. Characteristics of the experimental model. Exp. Biol. Med. 237 (5), 481–490.
Tramontina, A.C., et al., 2008. Secretion of S100B, an astrocyte-derived neurotrophic protein, is stimulated by fluoxetine via a mechanism independent of serotonin. Prog. Neuro-Psychopharmacol. Biol. Psychiatry 32 (6), 1580–1583.
Tramontina, F., et al., 2007. Immunoassay for glial fibrillary acidic protein: antigen recognition is affected by its phosphorylation state. J. Neurosci. Methods 162 (1–2), 282–286.
Vicente, E., et al., 2007. S100B levels in the cerebrospinal fluid of rats are sex and anaesthetic dependent. Clin. Exp. Pharmacol. Physiol. 34 (11), 1126–1130.
Wartchow, K.M., et al., 2016. Insulin stimulates S100B secretion and these proteins antagonistically modulate brain glucose metabolism. Neurochem. Res. 41 (6), 1420–1429.